Available online at www.sciencedirect.com

SciVerse ScienceDirect

Ceramics International 39 (2013) 8279–8285

CERAMICS INTERNATIONAL

www.elsevier.com/locate/ceramint

Aqueous tape casting of micro and nano YSZ for SOFC electrolytes

Tomas Baquero[a], Jairo Escobar[a], Jorge Frade[b], Dachamir Hotza[c,*]

[a]Group of Materials and Manufacture (CIPP-CIPEM), University of Los Andes (UNIANDES), Cra 1 No. 18A-12 Bogotá, Colombia
[b]DEMaC-CICECO, University of Aveiro, 3810-193 Aveiro, Portugal
[c]Group of Ceramic and Glass Materials (CERMAT), Federal University of Santa Catarina (UFSC), Department of Chemical Engineering, 88040-900 Florianópolis, SC, Brazil

Received 26 February 2013; received in revised form 3 March 2013; accepted 25 March 2013
Available online 10 April 2013

Abstract

Yttria-stabilized zirconia (YSZ) thick films with ~95% relative density were produced by aqueous tape casting to be used as electrolytes in solid oxide fuel cells (SOFC). Structural and morphologic properties of green and sintered bodies were analyzed starting from different particle size 8% yttria-stabilized zirconia powders. XRD showed the precursor powders to be single phase and nanocrystalline with composition within the expected range for cubic YSZ. Grain size distribution and specific area measurements confirmed the micrometer and nanometer range of the particles. Before casting, slurries were formulated based on rheological characterization, zeta potential and pH measurements. A relationship between starting powders, ceramic suspensions and sintered bodies was established and adapted to the tape casting process.

Keywords: A. Suspensions; A. Tape casting; Solid oxide fuel cells; Yttria-stabilized zirconia

1. Introduction

Fuel cells are electrochemical devices used for direct conversion of chemical energy to electrical energy. These technologies are silent, clean and efficient. They might be used for cogeneration of electricity and heat. The feasibility of fuel cells operation with different fuels is well established, including hydrogen and hydrocarbons [1], as well as renewable fuels such as methanol or ethanol. In this way, a fuel cell can be an alternative to internal combustion engines and turbines as the primary way to convert chemical energy into kinetic or electrical energy; hereby reducing greenhouse gas emissions and pollution [2–6]. Solid oxide fuel cells (SOFC) stand among other concepts of fuel cells for attaining very high efficiencies in cogeneration of electricity and heat with low environment impact. Greenhouse gases are eliminated when pure hydrogen is used, especially if solid oxide cells are used in reversible fuel and electrolysis modes [7].

A basic SOFC configuration consists of layers of anode, electrolyte and cathode, with additional interconnectors, supporting materials and sealants. In addition to performance and stability of individual cell components, the system must ensure chemical compatibility to avoid reactions between contacting cell components under firing conditions or during long term operation [8]. Thermo-chemical compatibility is also needed to minimize stresses [9] and risks of instantaneous failure or long term ageing. These issues are closely dependent on processing methods required to assemble the cells, which are comprised of a gas-tight solid electrolyte and highly porous electrodes.

Currently, studies are mainly aimed to develop alternative materials that help lowering operating temperatures to 500–800 °C and/or to obtain adequate and economic manufacturing methods in order to enhance prospects for commercial exploitation of these technologies [2–5]. Requirements for high purity materials are also an important cost factor. Nevertheless, the state-of-the-art materials show systematic degradation before the expected lifetime of fuel cells [10]. Thus, alternative concepts such as self healing with potential for long lasting effects have been considered [11].

The scope of the present work is focused on assessment of relevant parameters for producing aqueous cast tapes of YSZ to be used as SOFC electrolyte. This innovative approach is expected to yield a simple and mass production fabrication

*Corresponding author. Tel.: +55 48 3721 2518; fax: +55 48 3721 7615.
E-mail address: dhotza@gmail.com (D. Hotza).

0272-8842/$ - see front matter © 2013 Elsevier Ltd and Techna Group S.r.l. All rights reserved.
http://dx.doi.org/10.1016/j.ceramint.2013.03.097

method to replace costly processing and to avoid the use of hazardous solvents.

Tape casting is a process for manufacturing flat and thin (25–2000 μm) components with large surface areas. It consists mainly of a static blade with a moving carrier that takes the slip from a reservoir and leads it to a drying zone. The blade's height, controlled by a micrometer, determines the green tape thickness [12]. Tape casting is usually based on ceramic suspensions in organic liquids, whereas aqueous tape casting refers to the use of water-based ceramic suspensions. Aqueous tape casting, in spite of its contribution to minimize the environmental impact, is rarely considered due to drawbacks such as slurry sedimentation, foam generation during milling and low densities of green tapes [13].

2. Experimental procedure

Manufacturing ceramic tapes comprises three stages. The first one refers to the characterization of the ceramic powder, required to define the formulation of the ceramic slurries. The second stage refers to the stabilization through rheological studies and zeta potential measurements. The last stage includes casting and drying. After drying, green tapes are subjected to binder removal and sintering. In this section every stage is detailed.

2.1. Raw materials and characterization

Micrometric commercial 8% yttria-stabilized zirconia powders (Sigma Aldrich, USA), named YSZ-1, and YSZ nanometric powders (Innovnano, Portugal), named YSZ-2, were used.

Crystallinity and phase purity were investigated by X-ray diffraction with Cu Kα radiation (Philips X'Pert, The Netherlands). Particle size distribution as well as zeta potential measurements were carried out in a single equipment (zeta-nanoziser Zen 3600, Malvern, USA). BET adsorption method was performed to measure particle specific surface area. Finally, a scanning electron microscope (JEOL JSM-6390LV, Japan) was used to analyze morphology and size of the powders.

2.2. Slip design and stabilization

An experimental design of slurries was based on Taguchi's method [14], as a guideline for faster optimization. YSZ-1 studies were developed simultaneously by Moreno et al. [15]. Table 1 shows YSZ-2 formulations in %wt, and Table 2 shows YSZ-1 and YSZ-2 final formulations.

Based on this design, different aqueous slurries were prepared changing the amount of additives. In slurries A1, A2, and A3 the dispersant quantities were varied; in slurries B1 and B2 the amount of binder was varied; and in C1 and C2, the solid load and binder amounts were modified. Deionized water was added to complete 100%wt in every slip.

Ammonium polyacrylate (Darvan C, Vanderbilt, USA) was used as a dispersant and styrene acrylic copolymer (Mowilith LDM 6138, Clariant, USA) was added as a binder. A defoaming agent (DF002, Polymer Innovations, USA) was used to reduce foam generation during grinding. Moreover, isopropyl alcohol was employed to lower slip adherence to the carrier.

Table 1
YSZ-2 Composition of slurries in %wt.

Slurry	A1	A2	A3	B1	B2	C1	C2
Solid load	40	40	40	40	40	50	50
Binder	10	10	10	10	15	20	25
Dispersant	1.25	1.5	2	2	2	2	2
Surfactant	0.5	0.5	0.5	0.5	0.5	0.5	0.5
Defoaming agent	0.5	0.5	0.5	0.5	0.5	0.5	0.5
Isopropyl alcohol	1.5	1.5	1.5	1.5	1.5	1.5	1.5
Water	— — — — —		Balance		— — — — — — — —		

Table 2
Final YSZ-1 and YSZ-2 slurry compositions.

Slurry components	YSZ-1 [15]		YSZ-2	
	%wt	%vol	%wt	%vol
YSZ	55	58.25	50	51.20
Water	16.5	14.98	20.5	17.16
Dispersant	1	0.85	2	1.94
Binder	25	23.10	25	26.46
Surfactant	0.5	0.47	0.5	0.54
Defoaming agent	0.5	0.46	0.5	0.53
Isopropyl alcohol	1.5	1.89	1.5	2.16

Zeta potential measurements were performed to analyze colloidal stability as a function of pH. Rheology studies included flow curves at given shear rates, viscosity and effect of additives on the suspension behavior. Tests were done with a concentric cylinder viscometer (Haake VT550) at 25 °C, with sample rate of 200 data per min and shear rate from 1 to 600 or 1000 s^{-1} depending on the viscosity of each slurry. Every run was performed twice to identify thixotropy. Aging tests were carried out to evaluate slurries behavior after the evaporation of some additives. Three measurements were done: in the moment the slurry was ready for casting, and after 30 min and 1 h, respectively.

2.3. Tape casting

Ceramic powders, dispersant and solvent were mixed for 24 h in an alumina ball mill. Then, binder and surfactant were added and milled 30 min longer. Finally, the slurry was left to rest for 24 h for deairing.

A table top tape caster (TTC-1200, Mistler, USA) was used. A blade gap between 50 and 150 μm and a reservoir height of 10 mm were set. Carrier velocity was 60 mm/min. Tapes were dried at room temperature during 12 h.

2.4. Additives removal and tapes sintering

Thermogravimetric analysis at 5 °C/min and up to 800 °C (STA-409 CD, Netzsch, Germany) was performed to define the thermal cycles for green tapes.

Sintering temperature was set at 1600 °C for 3 h with a cooling rate of 10 °C/min. Initial tape dimensions were 60 mm × 30 mm × 55 ± 1 μm.

2.5. Characterization of sintered tapes

Microstructural characterization of sintered tapes was performed by image analysis of SEM microstructures (JEOL JSM-6390LV, Japan). Porosity was calculated with the computational tool ImageJ, following guidelines described in [16] to evaluate homogeneity, and grain size and shape.

3. Results and discussion

3.1. Characterization of raw materials

Fig. 1 shows the diffractograms of both YSZ materials with pure cubic phase. No other phase was detected. Fig. 2 shows curves of particle size distribution of the as-received YSZ powders. Both materials have a symmetrical distribution with a particle mean size of 0.56 μm for YSZ-1 and 0.24 μm for YSZ-2, with presence of agglomerates in YSZ-1 (~5.5 μm). However, it can be seen that YSZ-1 distribution is narrower than YSZ-2, and that YSZ-2 has particles with size between 40 to 80 nm.

Fig. 3 shows SEM micrographs of as-received powders, where the micrometric and nanometric scale of their particle sizes can be confirmed. Furthermore, in Fig. 3a, YSZ-1 agglomerated particles detected in particle distribution can be seen. Surface areas for YSZ-1 and YSZ-2 were 23.6 and 76.7 m^2/g, respectively. Those results indicate that different slurry formulations for each powder must be considered.

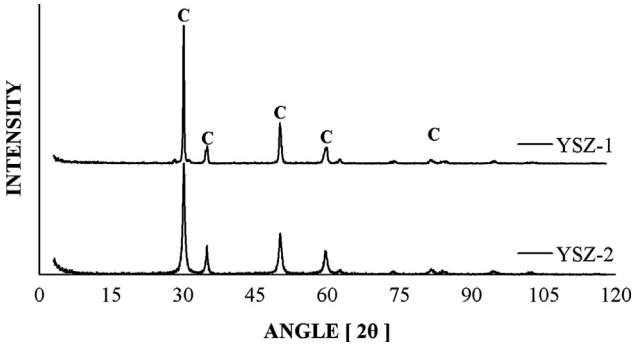

Fig. 1. YSZ-1 and YSZ-2 diffractograms.

3.2. Slip design and stabilization

Fig. 4 shows results of zeta potential measurements. Isoelectric point (zeta potential = 0) was found to be at pH ~8.2 for both powders. The slurries were set to pH 9.2 for YSZ-1 and 7.4 for YSZ-2 for further processing.

Zeta potential measurements emphasize the role of pH. Thus, slurry formulations were defined distant from isoelectric point to avoid flocculation. Moreover, it can be seen that

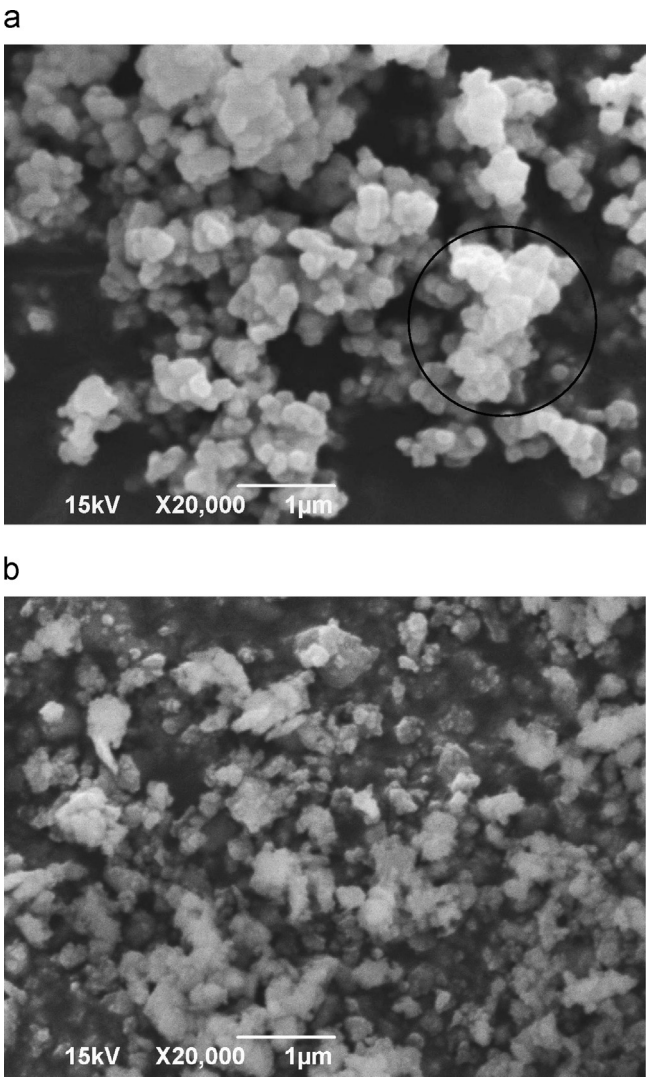

Fig. 3. Morphology of as-received (a) YSZ-1 and (b) YSZ-2 as observed by SEM.

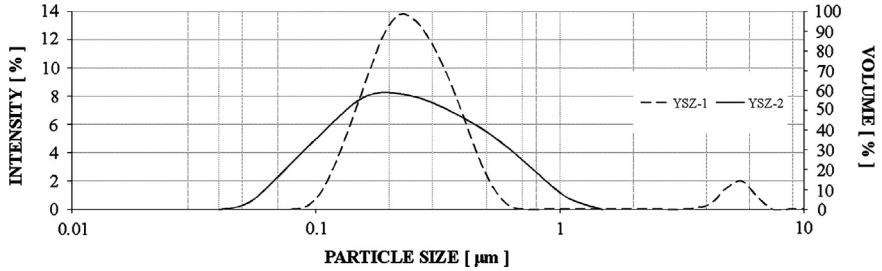

Fig. 2. Particle size distribution of as-received YSZ powders.

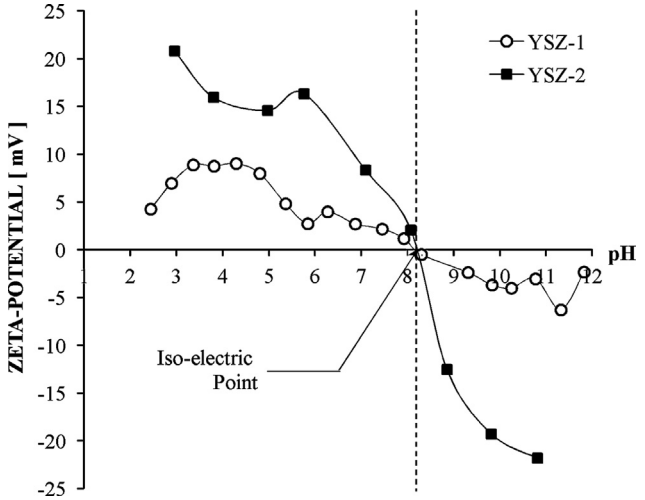

Fig. 4. Variation of Zeta potential with pH for YSZ-1 and YSZ-2 aqueous suspensions.

YSZ-2 suspensions tend to be more unstable than YSZ-1, because the latter zeta potential values change more sharply with pH variations.

Figs. 5–8 show rheological testing of different slurries. In all of them a pseudoplastic behavior with thixotropy was evidenced. Those conditions are desirable in tape casting because the slip viscosity decreases as shear stress increases [17].

3.2.1. Dispersant effect

Fig. 6 shows shear stress and viscosity curves as a function of shear rate for slurries A1, A2 and A3. As dispersant quantities increase, shear stress and viscosity values decrease. Regarding the measurements of A3, the dispersant amount was not increased, because an unstable slip could be obtained due to a pH close to the isoelectric point. The amount of dispersant used in A3 was set for further slips because of low values of shear stress favorable to tape casting process.

3.2.2. Binder effect

Fig. 5 shows shear stress and viscosity curves as a function of shear rate for slurries B1 and B2.

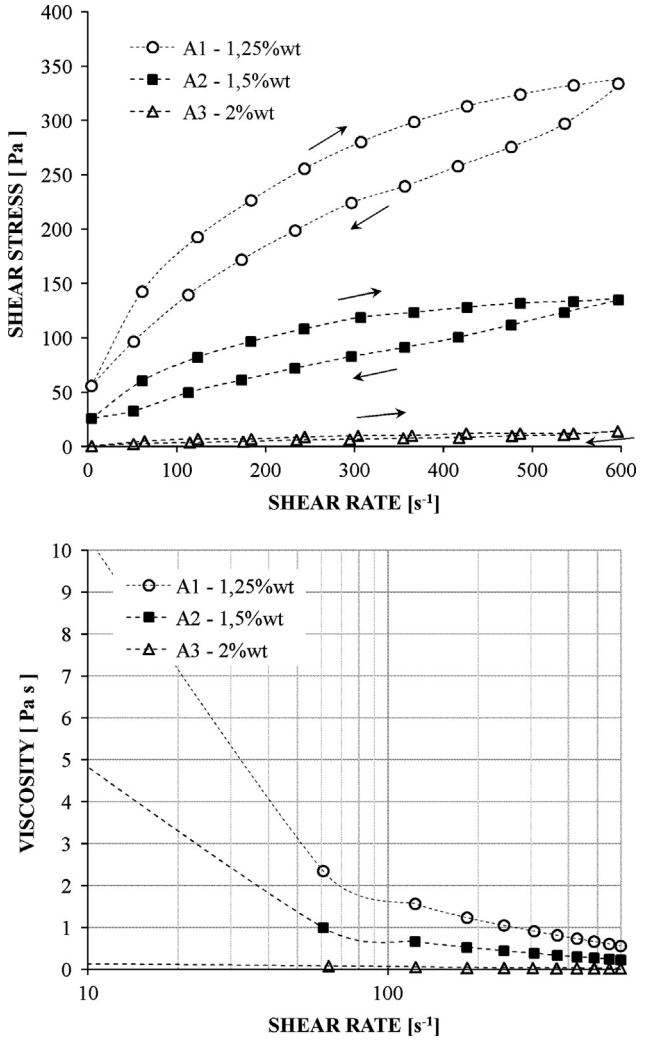

Fig. 5. Rheological behavior of A1, A2, and A3 slurries at different dispersant content.

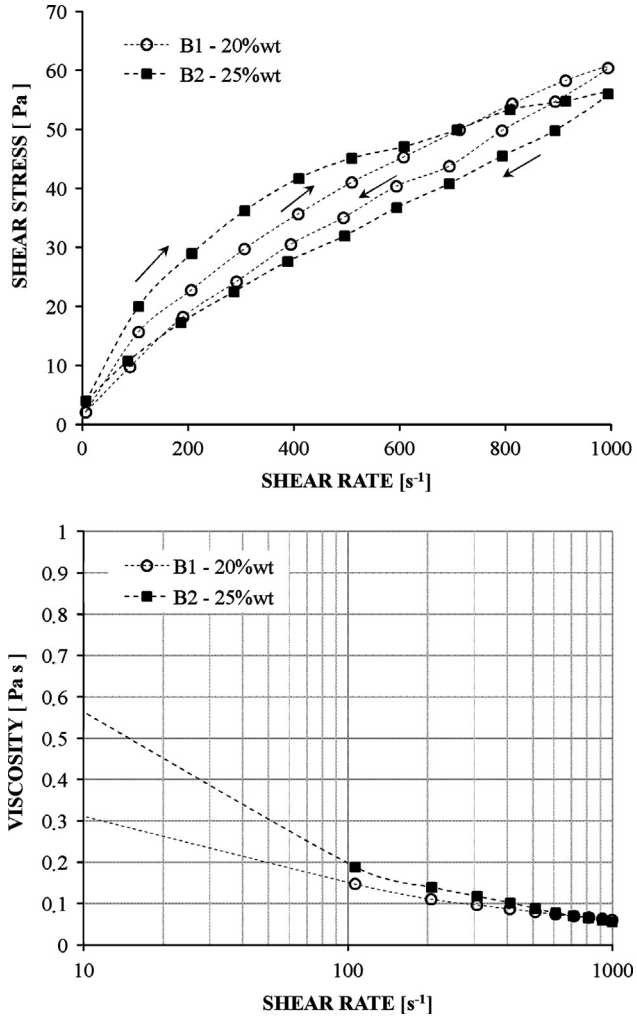

Fig. 6. Rheological behavior of B1 and B2 slurries at different binder content.

As long as the binder content was increased in slurries, shear stress and viscosity values increased in comparison with results in Fig. 5. This was expected because of the polymeric chains that characterize this additive, causing ceramic particles to restrict their movement in slurries when shear stresses are applied. Nevertheless, shear stress and viscosity values are among typical values reported in tape casting (0.1–1 Pa s at 100 s^{-1}). [18,19]

Slurries must fulfill permeability requirements in order to cover homogeneously the carrier during casting, and must also have a low surface adherence for an easy removal of the tapes when dried. [20] Tapes obtained with B1 and B2 slurries resulted to be very fragile and were impossible to remove from the carrier without cracking. For this reason it was decided to increase the amount of binder in C1 and C2 slurries.

Fig. 7 shows shear stress and viscosity curves as a function of shear rate for those slurries. Values for shear stress and viscosity were similar to the ones registered in Fig. 6. As binder content was increased with solid load in the slip, a steric repulsion may have been induced among the new powder particles due to the binder's polymeric chains. This may explain why the rheological properties values were alike in slurries B1, B2, C1 and C2 [21]. Tapes cast from C1 and C2 slurries were the most flexible of all samples. However, tapes related to C2 slip were removed easier from the carrier, so that this slip formula was selected for YSZ-2 powders. Table 2 shows the final formulations for both YSZ powders.

3.2.3. Aging effect

Fig. 8 shows the aging study results. As time passed, slurries presented higher values of viscosity and a yield stress was noticed at the beginning of the sampling. This meant that slurries changed from pseudoplastic to plastic (Bingham) behavior due to early evaporation of some additives in the slip. Moreover, sedimentation was observed in the slurries, which could induce the generation of agglomerates and flocks, affecting notably the quality of tapes.

3.3. Additives removal and tapes sintering

Based on thermogravimetric results, a plateau temperature was set at 500 °C during 1 h to guarantee the elimination of most of the organic additives. Total mass loss of organic components was found to be in the range of 300 to 500 °C.

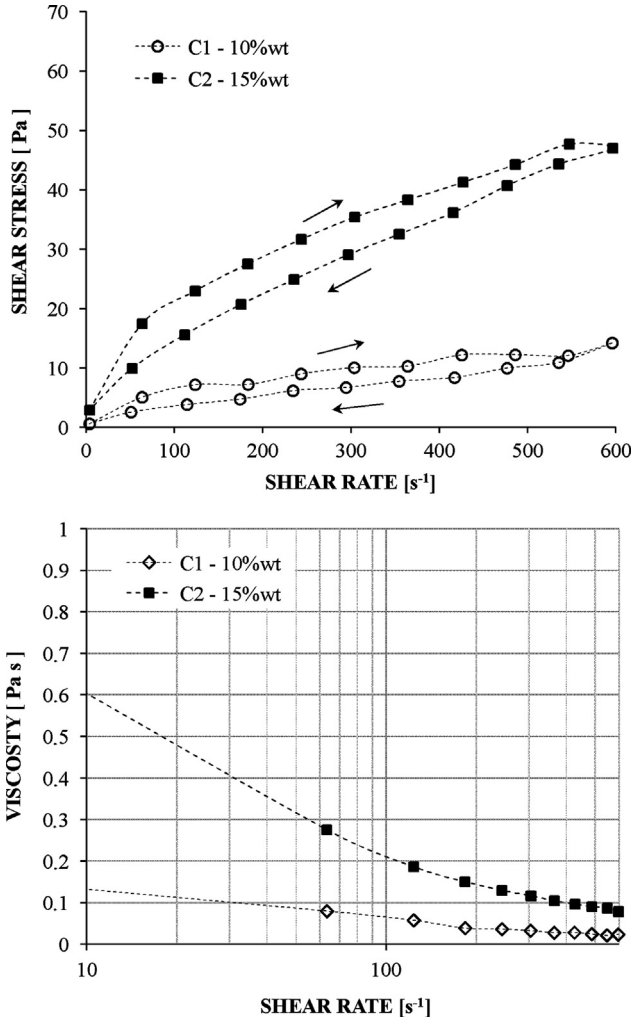

Fig. 7. Rheological behavior of C1 and C2 slurries at different solid-load and binder content.

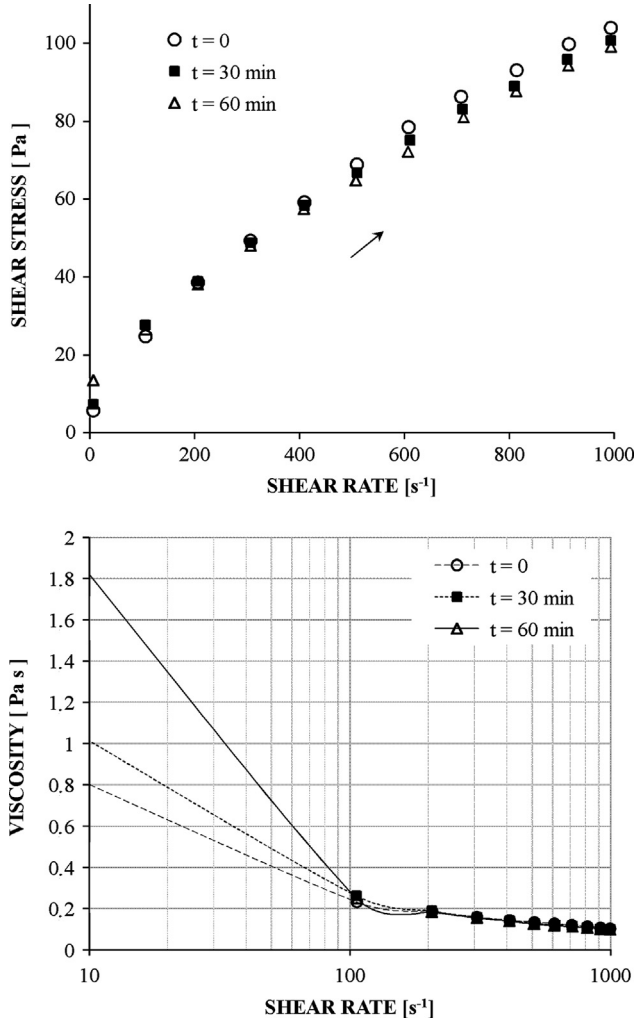

Fig. 8. Variation of rheological behavior with time of final YSZ-2 slurry.

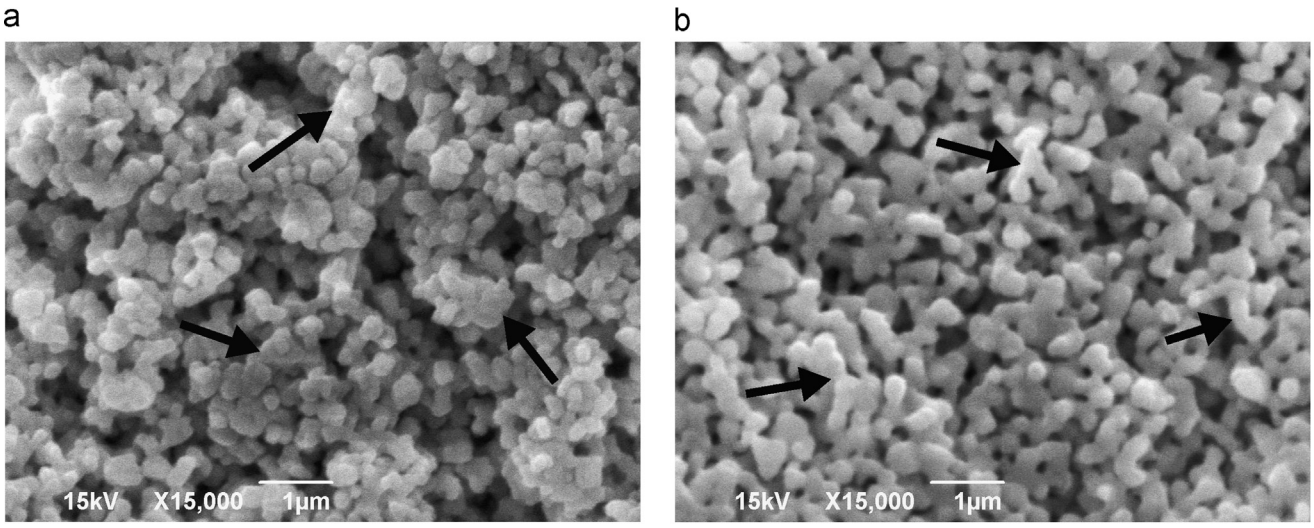

Fig. 9. SEM micrographs of presintered tapes at 1200°C of (a) YSZ-1 and (b)YSZ-2.

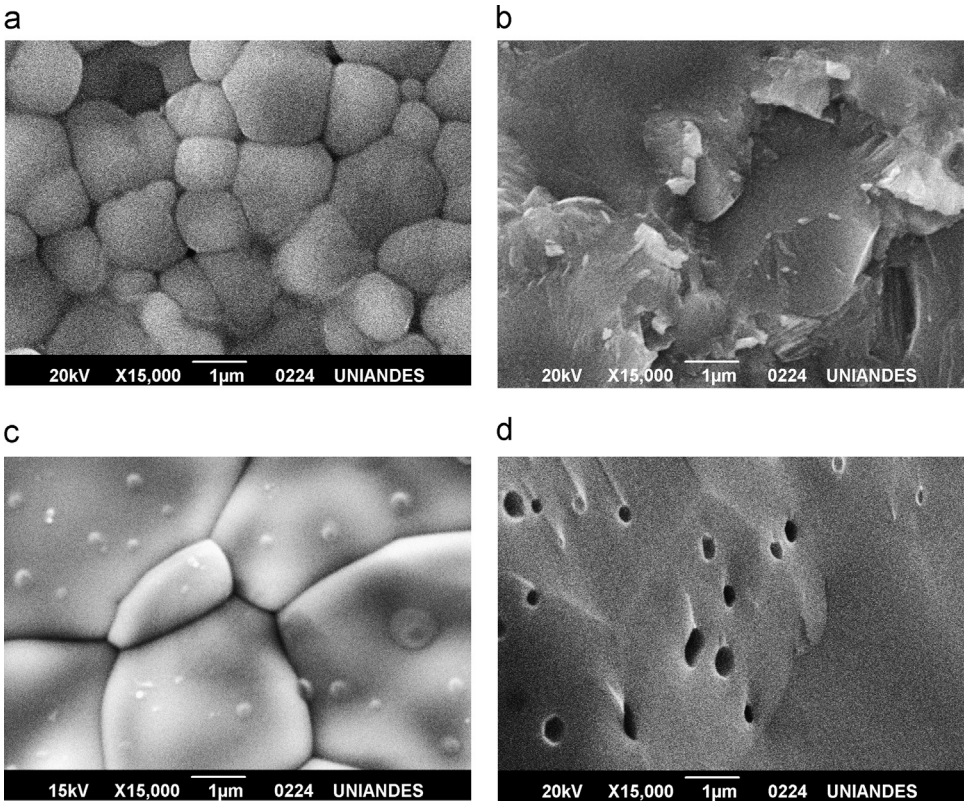

Fig. 10. SEM micrographs of sintered tapes at 1600 °C of (a) YSZ-1 surface, (b) YSZ-1 cross-section, (c) YSZ-2 surface (d) YSZ-2 cross-section.

Fig. 9 shows YSZ-1 and YSZ-2 tapes, pre-sintered at 1200 °C. The formation of necks and grain borders can be seen. In addition, significant porosity due to the additive removal can be found.

3.4. Characterization of sintered tapes

A dimensional change was observed in the tapes when removed from the furnace. An anisotropic shrinkage was confirmed after SEM analysis by the new measures of the tapes: 48 mm × 25 mm and 58 μm for YSZ-1; and 48 mm × 24mm and 40 μm for YSZ-2. Longitudinal and transverse shrinkages were ~20% and thickness reduction was ~30–55% regarding to initial dimensions. The latter contraction was higher probably because of the effect that the solvent has on the binder during the drying stage. Water evaporates from the surface, and as it rises from the carrier, it transports binder constantly. At the end, it results in a high concentration of binder molecules in the tape at the surface, which

are eliminated during sintering, causing higher dimensional change in this direction [17].

Fig. 10 shows the microstructural comparison of YSZ-1 and YSZ-2 sintered tapes. Fig. 10a shows microstructure for YSZ-1, where cubic and hexagonal grains of ~1–3 μm are predominant with a bimodal distribution. It can be stated that due to the concavity of the grains, they tend to shrink leading to pore generation (detected among grain borders) [22]. Fig. 10b shows cross section of YSZ-1 sintered tape where a fractured, relatively dense layer with low porosity can be observed.

Fig. 10c reveals YSZ-2 a microstructure dominated by typical, uniformly distributed hexagonal grains in the range of 2 to 5 μm [20,23]. Fig. 10d shows a cross section of YSZ-2 tape where a dense layer with 0.3 μm pores be seen. This porosity is due to the high reactivity of powders and high sintering temperature.

Porosity analysis showed that YSZ-2 tapes were denser than YSZ-1 despite the lower solid load. Relative density was found to be ~92.5% for YSZ-1 and ~94.5% for YSZ-2 in contrast to the green density of ~48% for both powders. This difference may be caused by the initial agglomerates in YSZ-1 powders, which under same sintering conditions, lead to a lower density. [19] Mercury porosimetry technique is recommended to obtain more accurate results.

4. Conclusions

Aqueous tape casting is a simple and adequate manufacturing method for production of YSZ electrolytes. Different YSZ precursor powders with differences in morphology and size distributions were used in order to confirm that process parameters can be adjusted to attain similar final results.

Thin and flexible green tapes were manufactured, validating the alternative use of aqueous suspensions. The process was controlled in all stages with careful attention to the drawbacks of using water in slips. Final slurry formulations were based on powder and rheological characterization.

Dense and homogeneous tapes with relative density close to 94.5% were obtained after sintering, meeting the morphological requirements of a dense electrolyte. A further electrical characterization is necessary to confirm the potential use of the obtained material as electrolyte in a solid oxide fuel cell.

Acknowledgment

Innovnano, Portugal, kindly offered YSZ powders for this study. PROSUL and EULANEST projects, financed by the Brazilian Agency CNPq, are gratefully acknowledged.

References

[1] B.C.H. Steele, Fuel cell technology: running on natural gas, Nature 400 (1999) 619–621.
[2] R. O'Hayre, Fuel Cell Fundamentals, 2nd ed., Wiley, Hoboken, NJ, 2009.
[3] C. Spiegel, Designing and Building Fuel Cells, McGraw-Hill, New York, 2007.
[4] S. Srinivasan, Fuel Cells: From Fundamentals to Applications, Springer, New York, 2006.
[5] J.H. Hirschenhofer, D.B. Stauffer, R.R. Engleman, M.G. Klett, Fuel Cell Handbook, 4th ed., Parsons, Morgantown, WV, 1998.
[6] D. Hotza, J.C. Diniz da Costa, Fuel cells development and hydrogen production from renewable resources in Brazil, International Journal of Hydrogen Energy 33 (2008) 4915–4935.
[7] M.A. Laguna-Bercero, Recent advances in high temperature electrolysis using solid oxide fuel cells: a review, Journal of Power Sources 203 (2012) 4–16.
[8] H. Yokokawa, Overview of intermediate-temperature solid oxide fuel cells, in: T. Ishiara (Ed.), Perovskite Oxides for Solid Oxide Fuel Cells, Springer, New York, 2009, pp. 17–43.
[9] J.R. Frade, Challenges imposed by thermochemical expansion of solid state electrochemical materials, in: J.T.S. Irvine, P. Connor (Eds.), Solid Oxide Fuel Cells—Facts and Figures, Springer, New York, 2013, pp. 95–120.
[10] T. Horita, H. Kishimoto, K. Yamaji, M.E. Brito, Y. Xiong, H. Okokawaa, Y. Hori, I. Miyachi, Effects of impurities on the degradation and long-term stability for solid oxide fuel cells, Journal of Power Sources 193 (2009) 194–198.
[11] T. Carvalho, E. Antunes, J. Calado, F.M. Figueiredo, J.R. Frade, Lanthanum oxide as a scavenging agent for zirconia electrolytes, Solid State Ionics 225 (2012) 484–487.
[12] B. Bitterlich, C. Lutz, A. Roosen, Rheological characterization of water-based slurries for the tape casting process, Ceramics International 28 (2002) 675–683.
[13] D. Hotza, P. Greil, Aqueous tape casting of ceramic powders, Materials Science and Engineering A202 (1995) 206–217.
[14] G. Taguchi, S. Chowdhury, Y. Wu, Taguchi's Quality Engineering Handbook, Wiley, Hoboken, NJ, 2005.
[15] V. Moreno, J.L. Aguilar, D. Hotza, 8YSZ tapes produced by aqueous tape casting, Materials Science Forum 727–728 (2012) 752–757.
[16] M.W. Quintero, J.A. Escobar, A. Rey, A. Sarmiento, C.R. Rambo, A.P.N. Oliveira, D. Hotza, Flexible polyurethane foams as templates for cellular glass-ceramics, Journal of Materials Processing 209 (2009) 5313–5318.
[17] R. Mistler, E. Twiname, Tape Casting: Theory and Practice, The American Ceramic Society, Westerville, 2000.
[18] F. Doreau, G. Tarí, C. Pagnoux, T. Chartier, M.F. Ferreira, Processing of aqueous tape-casting of alumina with acrylic emulsion binders, Journal of the European Ceramic Society 18 (1998) 311–321.
[19] A. Mukherjee, B. Maiti, A. Das Sharma, R.N. Basu., H.S. Maiti, Correlation between slurry rheology, green density and sintered density of tape cast yttria stabilized zirconia, Ceramics International 27 (2001) 731–739.
[20] F. Snijkers, A. de Wilde, S. Mullens, J. Luyten, Aqueous tape casting of yttria stabilized zirconia using natural product binder, Journal of the European Ceramic Society 24 (2004) 1107–1110.
[21] S.Y. Gómez, O. Alvarez, J. Escobar, J.B. Rodrigues Neto, C. Rambo, D. Hotza, Relationship between rheological behaviour and final structure of Al_2O_3 and YSZ foams produced by replica, Advances in Materials Science and Engineering 549508 (2012) 1–9.
[22] J. Reed, Principles of Ceramics Processing, 2nd ed., Wiley, New York, 1995.
[23] P. Timakul, S. Jinawath, P. Aungkavattana, Fabrication of electrolyte materials for solid oxide fuel cells by tape-casting, Ceramics International 34 (2008) 867–871.